Korean J. Chem. Eng., 33(11), 3128-3133 (2016)
DOI: 10.1007/s11814-016-0143-1

pISSN: 0256-1115
eISSN: 1975-7220

Thermogravimetric characteristics of *α-cellulose* and decomposition kinetics in a micro-tubing reactor

Seung-Soo Kim*, Hoang Vu Ly*, Byung Hee Chun*, Jae-Heung Ko,†, and Jinsoo Kim***,†**

*Department of Chemical Engineering, Kangwon National University, 346 Joongang-ro, Samcheok, Gangwon-do 25913, Korea
**Department of Plant and Environmental New Resources, Kyung Hee University,
1732 Doegyeong-daero, Giheung-gu, Yongin, Gyeonggi-do 17104, Korea
***Department of Chemical Engineering, Kyung Hee University,
1732 Doegyeong-daero, Giheung-gu, Yongin, Gyeonggi-do 17104, Korea
(*Received 9 March 2016 • accepted 25 May 2016*)

Abstract−The pyrolysis characteristics and kinetics of α-cellulose were investigated using thermogravimetric analyzer (TGA) and micro tubing reactor, respectively. Most of the α-cellulose decomposed between 250 and 400 °C at heating rate of 5-20 °C/min. The apparent activation energy was observed in the range of 263.02 kJ mol^{-1} to 306.21 kJ mol^{-1} at the conversion of 10-80%. The kinetic parameters were determined by nonlinear least-squares regression of the experimental data, assuming first-order kinetics. It was found from the kinetic rate constants that the predominant reaction pathway was **A**(α-cellulose) to **B**(bio-oil) rather than **A**(α-cellulose) to **C**(gas; C_1-C_4) and/or to **B**(bio-oil) to **C**(gas; C_1-C_4) at temperatures of 340-360 °C.

Keywords: Woody Biomass, α-Cellulose, Pyrolysis, Lump Kinetic Model, Thermogravimetric Analysis

INTRODUCTION

Biomass has been recognized as a potential renewable energy source to replace fast depleting fossil fuels [1-3]. Pyrolysis is considered as one of the most promising thermochemical conversion techniques for biomass conversion. However, pyrolysis is a very complex process with a series of reactions which can be influenced by many factors [3-5]. Moreover, the pyrolysis bio-oil is essential to be upgraded to improve its quality for use directly as fuel, due to its high oxygen, acidity and low heating value [6]. Therefore, a thermogravimetric analysis (TGA) of the kinetics of pyrolysis of biomass is needed in order to understand the pyrolysis characteristics of biomass.

As lignocellulosic biomass is made up of 20-40% of hemicellulose, 40-60% of cellulose, and 10-25% of lignin, its pyrolysis can be considered as the superposition of the three main components [5, 7,8]. It is essentially important to study the pyrolysis characteristics of the main component of lignocellulosic biomass for a better understanding of biomass thermochemical conversion [9].

Cellulose is the main constituent of biomass as well as the most abundant biopolymer on Earth [10] with approximately 1.5×10^{12} tons of cellulose produced annually [11]. As cellulose is the primary component in lignocellulosic biomass, a thorough knowledge of the pyrolysis characteristics of cellulose is required for the proper design and operation of the pyrolysis conversion systems.

Kim et al's [12] research works in understanding cellulose structure and applications have been well reviewed. Catalytic conversion of cellulose has been researched to get value-added chemicals such as 5-hydroxymethylfurfural [13]. Thermogravimetric analysis (TGA) has been widely used to investigate the conditions of pyrolysis as well as development of kinetic models for cellulose pyrolysis. In general, pyrolysis models can be divided into two categories [14]. The first is a global decomposition mechanism where a single first order irreversible reaction is used to describe the experimentally observed weight loss rate [15-17]. A parallel reaction scheme based on the Broidio-Shafizadeh model has been widely accepted [18]. According to this mechanism, cellulose is first depolymerized to 'active cellulose', which has a degree of polymerization of around 200-250 monomer units. This initial reaction is then followed by decomposition into 'char' and 'volatile' products by several competitive reactions. Alternatively, a second semi-global multi-step type mechanism has been presented by several researchers, which exclusively considers primary and secondary reactions occurring during pyrolysis [18,19]. This second type of model appears to give a reasonable description of experimental results and has been used to predict the product yields of bio-oil, char and gas fractions resulting from primary as well as secondary reactions [20].

Most of the kinetic models introduced above classified the pyrolysis products into bio-oil, char and gas, based on mass loss measurements in TGA experiments or TGA coupled with GC/MS. Kinetic models by thermogravimetric analysis use weight loss of samples by increasing temperature [21]; thus this method does not use the fractionated components of product.

In this work, however, liquid product and gas product were fractionated by weighing after specific pyrolysis temperature and time in a micro tubing reactor. The kinetic reaction constants were eval-

†To whom correspondence should be addressed.
E-mail: jhko@khu.ac.kr, jkim21@khu.ac.kr
‡This article is dedicated to Prof. Sung Hyun Kim on the occasion of his retirement from Korea University.

uated by applying a lumped model based on actual mass loss of *α*-cellulose, gas product, and liquid product, respectively, after pyrolyzing *α*-cellulose in a micro-tubing reactor. The kinetic parameters from a lumped kinetic model were also calculated. A kinetic analysis was performed for better understanding the characteristics and the reaction mechanisms of the *α*-cellulose pyrolysis.

EXPERIMENTAL SECTION

The cellulose used in this study was *α*-cellulose (C8002), purchased from Sigma-Aldrich Co. It was fibrous form with a density of 0.60 g/cm^3.

Thermogravimetric analysis of the *α*-cellulose sample involved using a TGA (TA Instrument, Q50). A sample mass of 20.0±1.0 mg was used for the thermogravimetric analysis in each experiment. Nitrogen was used as a carrier gas, at a flow rate of 25 mL/min. The heating rates were controlled at 5, 10, 15 and 20 °C/min from 20 °C to 800 °C.

The pyrolysis of *α-cellulose* samples was carried out in a tubing reactor (ϕ22 mm×110 mm). The system consisted of a salt bath, a temperature controller, a mechanical stirrer and a reactor made of tubing with an inner volume of 39 ml. A sample mass of 3 g was used in each experimental run. The molten salt bath, which has excellent heat transfer properties, was composed of a eutectic salt of KNO_3 (59 wt%) and $Ca(NO_3)_2$ (41 wt%) [22-25]. Based on data from the differential thermogravimetric (DTG) curves, the pyrolysis temperatures of 340 °C, 350 °C, and 360 °C at molten salt bath were selected along with heating rates of 5, 10, 15 and 20 °C/min. First, the tubing reactor, which contained 3 g of the *α*-cellulose samples, was placed into the molten salt bath. The reaction time of the sample was varied from 1 min to 4 min at each pyrolysis temperature (340 °C, 350 °C, and 360 °C). After reaction, the reactor was taken out from the bath and cooled to room temperature. The reaction products were analyzed by weighing gas, oil, and solid products. After cooling, the tubing reactor was opened to allow gas to be gently released. The yield of gas, defined as (gas weight)×100/(feed weight), was obtained by weighing the tubing reactor before and after the gas release. The other pyrolyzed products were separated into bio-oil (acetone soluble) and solid (acetone insoluble) using a solvent extraction technique. The solid yield is defined as (weight of acetone insoluble)×100/(weight of feed), while the bio-oil is defined as (100-gas yield-solid yield). The solid was separated using 0.45 μm micro filter paper.

The pyrolysis bio-oil was analyzed by using GC-MS (Agilent 7890A) with a capillary column of HP-5MS (30 m×0.25 mm×0.25 μm). High purity helium was used as a carrier gas with gas flow rate of 1.0 ml/min. The temperature of GC injector was kept at of 280 °C, with injection volume of 1 μL. The GC oven was programmed from initial temperature of 40 °C to 200 °C with heating rate 5 °C/min, held for 5 min, then to 300 °C at heating rate 10 °C/min, held for 5 min.

RESULTS AND DISCUSSION

1. Thermogravimetric Analysis

The results of thermogravimetric experiments for the *α*-cellulose are expressed as a function of the conversion X, which is defined as

$$X = \frac{W_0 - W}{W_0 - W_\infty} \quad (1)$$

where W_0 is the initial mass of the sample, W is the mass of the pyrolyzed *α*-cellulose sample, and W_∞ is the final residual mass after thermogravimetric analysis.

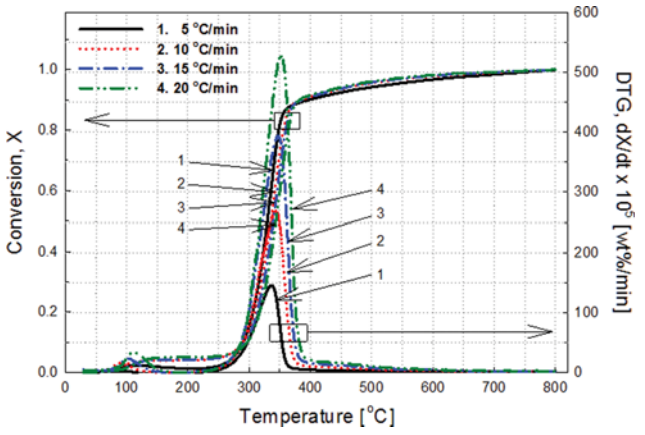

Fig. 1. TG and DTG curves illustrating the effect of the pyrolysis rate of *α-cellulose* at different heating rates of 5, 10, 15, and 20 °C/min.

The degrees of conversion for the *α*-cellulose and DTG curves are shown as a function of temperature in Fig. 1 at various heating rates of 5, 10, 15, and 20 °C/min. At temperatures lower than 150 °C, the small change in conversion of the samples is attributed to vaporization of the moisture attached to the surfaces of the samples. As shown in the Fig. 1, the *α*-cellulose samples started to decompose at 250 °C. The TGA graphs at the different heating rates of 5, 10, 15, and 20 °C/min showed similar results, shifting slightly toward the right with increasing heating rate. The TGA curves of the *α*-cellulose samples showed one weight loss step, with major decomposition occurring between 247 °C and 382 °C depending on heating rates. It is in good agreement with the literature data [22,26,27]. Yang et al. [9] reported that cellulose pyrolysis mainly occurred between 315 °C and 400 °C at the heating rate of 10 °C/min in nitrogen atmosphere, which is consistent with our result. Ouajai and Shanks studied thermal degradation of hemp cellulose by TG and DTG analysis after chemical treatment [27]. They reported that hemp cellulose decomposed at about 390-400 °C at the heating rate of 20 °C in nitrogen atmosphere. In contrast, hemicellulose and lignin of hemp were mainly decomposed at ca. 220 °C and 315-400 °C, respectively, at various heating rates of 5-20 °C/min [26].

The differential rate of conversion, dX/dt, was obtained from differential thermogravimetric analysis (DTG) at various heating rates of 5, 10, 15, and 20 °C/min (Fig. 1). The DTG curve at each heating rate has two extensive peaks, occurring between 20 °C and 400 °C. The first small peaks occurring lower than 150 °C are corresponding to vaporization of the moisture on the surface of sample, and the second large peaks between 247 °C and 382 °C are attributed to decomposition of the *α*-cellulose. The maximum rate

of dX/dt in the DTG curves (T_{max}) increased with increasing heating rate. As shown in Fig. 1, the maximum rate of decomposition tends to increase at higher heating rates because there is more thermal energy to facilitate better heat transfer between the surroundings and the insides of the samples [28]. The maximum point rates of decomposition in the DTG curves occurred at 334, 341, 347, and 352 °C, respectively, at heating rates of 5, 10, 15, and 20 °C/min. The results are in good agreement with the findings of Yang et al. [9]. They reported that the temperature of maximum weight loss rate for cellulose was 355 °C at the heating rate of 10 °C/min.

2. Kinetic Parameters of the Pyrolysis of α-Cellulose

The TGA graph was analyzed to determine the kinetic parameters of α-cellulose pyrolysis, including the activation energy and the Arrhenius frequency. The differential method was used to determine the pyrolysis kinetic parameters from the thermogravimetric data as below [22,29-31]:

$$\ln\left(\frac{dX}{dt}\right) = \ln(AX^n) - \frac{E}{RT}\frac{1}{} \quad (2)$$

where E is the activation energy, A is the pre-exponential factor, and n is the reaction order.

The activation energy, E, based on Eq. (2), can be determined from plot of ln(dX/dt) vs. 1/T. Fig. 2 shows the plots of ln(dX/dt) vs. 1/T at various conversions ranging from 10% to 80%, resulting in a family of parallel straight lines with a slope of −E/R. When the conversion of the α-cellulose was 20%, for example, the corresponding temperatures were 305.9 °C, 309.8 °C, 313.0 °C, and 317.3 °C for heating rates of 5, 10, 15, and 20 °C/min, respectively. At these temperatures, the values of ln(dX/dt) were −7.24, −6.68, −6.25, and −6.01 for heating rates of 5, 10, 15, and 20 °C/min, respectively. From the slope of ln(dX/dt) vs. 1/T for the 20% conversion, the activation energy was calculated to be 310.97 kJ/mol. The intercept, ln(A·X^n), can be obtained from Fig. 2 at each conversion. When the apparent order of reaction (n) is assumed to be 0, 1 or 2, the pre-exponential factor (A) can be obtained from Eq. (3).

$$\ln(A\cdot X^n) = \ln A + n\ln(X) \quad (3)$$

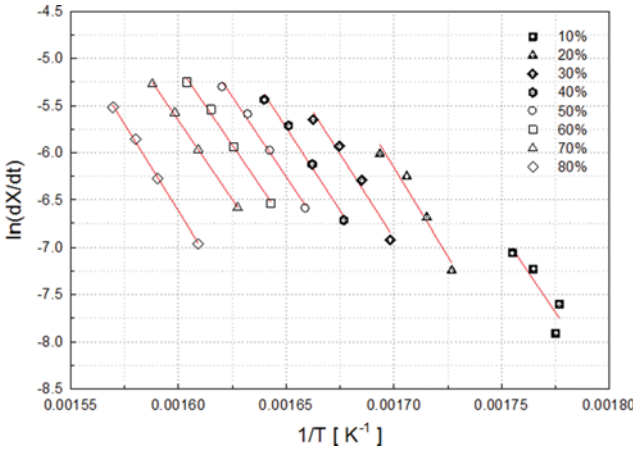

Fig. 2. Application of Eq. (2) with heating rates of 5, 10, 15, and 20 °C/min where the conversion values ranged from 10-80%.

The moisture on the surfaces of the α-cellulose was vaporized at a temperature lower than 150 °C, as shown in Fig. 1. Thus, the activation energy at the 5-10% conversion level was not the pyrolysis of α-cellulose but the vaporization of moisture. The carbohydrate was mainly decomposed at the temperature lower than 350 °C; after that, the further devolatilization reaction of charcoal of the α-cellulose proceeded. The activation energy for the pyrolysis of α-cellulose ranged from 263.02 to 306.21 kJ/mol, at the conversion of 10-80%. Vamvuka et al. reported that the activation energy for cellulose was in the range of 145-285 kJ/mol [32]. Wang et al. used the distributed activation energy model to study the pyrolysis kinetics, and calculated the activation energy values of cellulose in the range from 142.6 to 167.7 kJ/mol [33].

In our previous works, we investigated thermogravimetric characteristics of pine trees and oak trees, which are representative woody biomass of conifer and broad-leaved tree, respectively [22,24]. The activation energies of pine and oak trees were in the range of 229.98-246.43 kJ/mol and 238.28-384.34 kJ/mol, respectively, at the conversion of 10-80%. Considering that cellulose is the major component of these trees, the activation energies of α-cellulose in the range of 263.02 to 306.21 kJ/mol are reasonable.

Table 1 shows the apparent activation energies and pre-exponential factors calculated using Eq. (2) and Eq. (3) based on Fig. 2, assuming a zeroth, first or second order reaction. The pre-exponential factors were between 10^{20} and 10^{24} s^{-1}, when the conversion was between 10% and 80%.

3. Bio-oil Composition

The bio-oil obtained from α-cellulose pyrolysis at 360 °C for 4 min was analyzed with GC-MS (Agilent 7890A), and the data are presented in Table 2. Two major constituents of the bio-oil are 2-furancarboxaldehyde (46.3%) and 5-methyl-2-furancarboxaldehyde (15.4%).

Park et al. studied fast pyrolysis of Oriental white oak in a fluidized bed, and then analyzed bio-oil [34]. Biomass such as Oriental white oak mainly consists of cellulose, hemicelluloses and lignin. Three main components are produced, such as bio-oil, biochar and non-condensable gases, from the fast pyrolysis of lignocellulosic bio-

Table 1. Calculated kinetic parameters for the pyrolysis of α-cellulose

		Conversion (%)							
		10	20	30	40	50	60	70	80
E_a (kJ/mol)		263.02	310.97	296.88	292.0	282.21	278.96	273.64	306.21
n	0th	1.16×10^{21}	8.67×10^{24}	2.29×10^{23}	4.75×10^{22}	4.04×10^{21}	1.28×10^{21}	2.55×10^{20}	5.21×10^{22}
	1st	1.15×10^{22}	4.34×10^{25}	7.61×10^{23}	1.19×10^{23}	8.05×10^{21}	2.13×10^{21}	3.65×10^{20}	6.49×10^{22}
	2nd	1.15×10^{23}	2.53×10^{24}	2.53×10^{24}	2.98×10^{23}	1.61×10^{22}	3.55×10^{21}	5.23×10^{20}	8.09×10^{22}

Table 2. Bio-oil analysis from the pyrolysis of α-cellulose: 360 °C, 4 min

RT (min)	Composition	Area %
3.199	2-Amino-1-butanol	4.28
3.957	2- Furancarboxaldehyde	46.31
5.791	Ethenyl ester propanoic acid	3.38
5.843	5-Methyl-2- Furancarboxaldehyde	15.42

Table 3. Effects of the pyrolysis conditions on the yields of oil, gas, and char (wt%) for α-cellulose in the micro-tubing reactor

	Reaction time (min)			
	1	2	3	4
Pyrolysis at 340 °C				
Gas (wt%)	0.59	5.67	14.64	15.80
Oil (wt%)	14.23	33.79	39.27	47.26
Solid (wt%)	85.18	60.54	46.09	36.94
Pyrolysis at 350 °C				
Gas (wt%)	0.70	6.71	14.0	16.15
Oil (wt%)	16.56	34.29	39.26	46.58
Solid (wt%)	82.74	59.0	46.74	37.27
Pyrolysis at 360 °C				
Gas (wt%)	1.80	12.75	15.07	16.76
Oil (wt%)	17.58	43.44	47.63	46.61
Solid (wt%)	80.62	43.81	37.30	36.63

mass. Bio-oil contains a great deal of oxygenated compounds; thus hydrodeoxygenation of those of compounds has been researched to upgrade its quality [35,36]. Biochars derived from biomass can be used for heavy metal removal [37]. The major compounds in the bio-oil from the fast pyrolysis of Oriental white oak were phenolic compounds, including cresols, guaiacols, eugenols, ayringols and their derivatives, as well as ketones and aldehydes. Ross et al. reported that lignin pyrolysis was known to produce mainly phenolic compounds [38].

In this work, 2-furancarboxaldehyde showed the highest selectivity among the produced compounds. Unlike woody biomass, α-cellulose did not contain as much phenolic compounds because of the absence of lignin.

4. Pyrolysis Mechanism for α-Cellulose

The effects of the pyrolysis temperature and reaction time for α-cellulose on the product yield were systematically investigated. The yields of oil, gas, and solid as a function of the pyrolysis conditions are shown in Table 3. The results clearly show the effects of the pyrolysis temperature and reaction time on the product yields. The yields of oil and gas were in the range of 14.23-47.26 wt% and 0.59-16.76 wt%, respectively, at the investigated conditions, while the yield of solid was higher than 36 wt% under the same experimental conditions. When pine tree was pyrolyzed at similar conditions, the yields of oil, gas and char were in the range of 4.03-25.57 wt%, 4.16-21.71 wt% and 53.45-91.63 wt%, respectively [22]. This difference is attributed to the compositions of pine tree, consisting of hemicellulose and lignin as well as cellulose.

To simplify the kinetic model of the experimental data, fractions of gas, oil, and solid were considered, and the kinetic model of the pyrolysis of α-cellulose was assumed for two groups of series

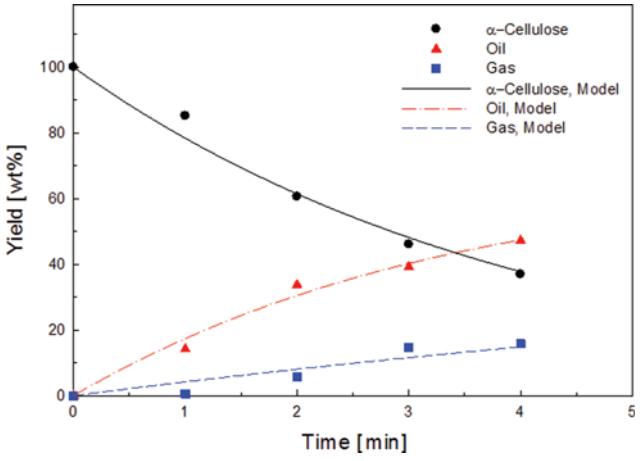

Fig. 3. Effect of reaction time on the product distribution for α-cellulose at 340 °C.

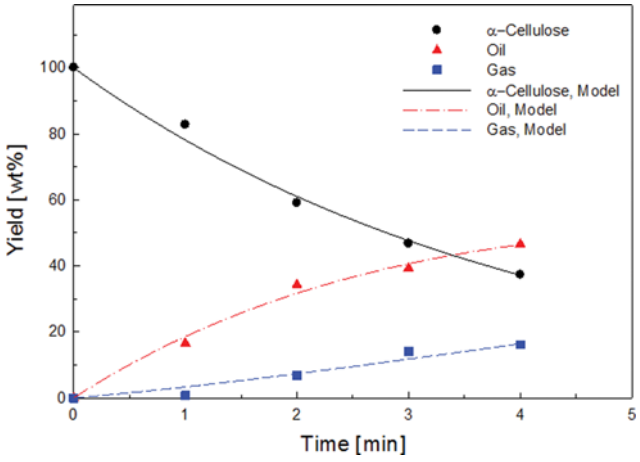

Fig. 4. Effect of reaction time on the product distribution for α-cellulose at 350 °C.

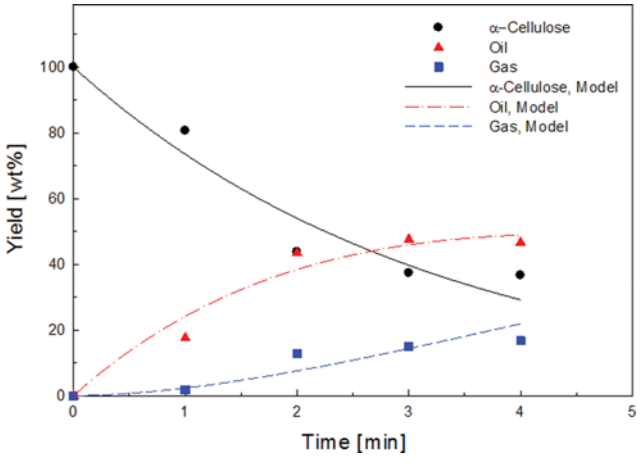

Fig. 5. Effect of reaction time on the product distribution for α-cellulose at 360 °C.

and parallel reactions. Figs. 3-5 show the yields of oil, gas, and solid as a function of reaction time at pyrolysis temperatures of 340 °C, 350 °C, and 360 °C, respectively. The initial fraction of α-cellulose was considered 100 wt%. The fraction of α-cellulose decreased with increasing reaction time at a fixed pyrolysis temperature, while the fractions of gas and oil increased with increasing reaction time at the same pyrolysis temperature. When the reaction time was over 3 min at any pyrolysis temperature, the yields of gas remained essentially constant.

The pyrolysis mechanisms assumed for the kinetic model development in our previous study are shown below [22,24].

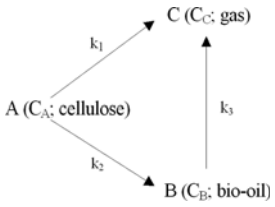

(4)

Based on Eq. (4), the kinetic equations for the reaction in terms of yields for cellulose (C_A), bio-oil (C_B) and gas (C_C) are as follows:

$$C_A = C_{A_0}\exp[-(k_1+k_2)t] \tag{5}$$

$$C_B = C_{B_0} + k_2 C_{A_0}\left(\frac{\exp[-(k_1+k_2)t]}{k_3-(k_1+k_2)} - \frac{\exp(-k_3 t)}{k_3-(k_1+k_2)}\right) \tag{6}$$

$$C_C = C_{A_0} - C_A - C_B \tag{7}$$

The reaction rate constants of k_1, k_2, and k_3 were obtained by applying an optimization procedure (Levenberg-Marquardt method) to the values of each component product at 340 °C, 350 °C and 360 °C. The method of parameter measurement can be mathematically formulated into the following constrained nonlinear optimization program:

$$\text{minimize } S = \sum_{i=1}^{N}(Y_{calculated,\,i} - Y_{experimental,\,i})^2 \tag{8}$$

where $Y_{calculated,\,i}$ and $Y_{experimental,\,i}$ refer to the value calculated by Eqs. (5)-(7) and the experimental values at a given pyrolysis temperature and time of reaction, respectively.

The reaction rate constants were estimated by applying Eq. (8) to the results shown in Figs. 3-5. The calculated reaction rate constants for the pyrolysis of α-cellulose are shown in Table 4. The reaction rate constants of k_2, and k_3 increased with increasing pyrolysis temperature from 340 °C to 360 °C, whereas k_1 decreased. The reaction rate constant of k_2 (α-cellulose→bio-oil) shows the highest value compared with k_3 (bio-oil→gas) and k_1 (α-cellulose→gas) values at each temperature. The ratio of k_2/k_3 at the reaction temperature of 340 °C, 350 °C and 360 °C was 6.38, 2.77 and 1.95, respectively. Obtained results suggest that the predominant reaction pathway of the pyrolysis of α-cellulose was from A to B rather than from A to C and/or B to C. This result is similar to the results obtained from the pyrolysis of woody biomass such as oak trees, where k_2 was higher than k_3 [24]. In the case of pine trees, k_1 was higher than k_2 and k_3 [22]. First-order lumped kinetics provide an excellent fit for the products obtained from α-cellulose at 340 °C, 350 °C and 360 °C. Thermogravimetric analysis of the α-cellulose was used to investigate the pyrolysis characteristics and to calculate the global kinetic parameters such as activation energy. The purpose of performing a kinetic analysis was to better understand the pyrolysis characteristics of α-cellulose, which is the major component of woody biomass. The lumped reaction scheme proposed can be proved by the pyrolysis mechanism of α-cellulose in Eqs. (5)-(7). This mechanism is in agreement with experimental results and accounts for the formation of the final products.

Table 4. Reaction rate constants (min^{-1}) for the pyrolysis of *α-cellulose*

Temperature (°C)	Rate constant (min^{-1})		
	k_1	k_2	k_3
340	0.0443	0.1992	0.0312
350	0.0288	0.2184	0.0788
360	0.0037	0.3041	0.1556

CONCLUSION

The global kinetic parameters for α-cellulose pyrolysis, including the apparent activation energies, were determined by the differential method. The activation energy of the pyrolysis of the α-cellulose was between 263.02 kJ/mol and 306.21 kJ/mol at the conversion range of 10-80%. The composition of bio-oil from the α-cellulose showed the highest selectivity of 46.3% for 2-furancarboxaldehyde when pyrolysis was at 360 °C for 4 min in the micro tubing reactor. The proposed lumped kinetic model matched well with the experimental results, and the kinetic rate constants suggest a predominant reaction pathway from α-cellulose to bio-oil rather than from α-cellulose to gas and/or bio-oil to gas.

ACKNOWLEDGEMENT

This research was supported by the Basic Science Research Program through the National Research Foundation of Korea (NRF) funded by the Ministry of Education, Science and Technology (NRF-2014R1A1A4A01008538) and the Ministry of Science, ICT & Future Planning (NRF-2014R1A5A1009799).

NOMENCLATURE

A : pre-exponential factor [s^{-1}]
E : activation energy [kJ mol^{-1}]
k : pyrolysis rate constant [min^{-1}]
n : reaction order
R : gas constant [8.314 J g·mol^{-1} K^{-1}]
t : pyrolysis time [min]
T : absolute temperature [K]
W : weight of sample at time t [g]
W_0 : initial weight of sample [g]
W_t : final weight of sample [g]
X : conversion of samples
T_{max} : maximum rate of dX/dt in the DTG curves
k_1, k_2, k_3 : reaction rate constants [min^{-1}]

C_A, C_B, C_C : yields of reactant and product [wt%]

REFERENCES

1. M. Jefferson, *Renew. Energy*, **31**, 571 (2006).
2. P. S. Nigam and A. Singh, *Prog. Energy Combust.*, **37**, 52 (2011).
3. S. H. Park, H. J. Cho, C. Ryu and Y. K. Park, *J. Ind. Eng. Chem.*, **36**, 314 (2016).
4. A. Demirbaş, *Fuel*, **80**, 1885 (2001).
5. J. J. Manya, E. Velo and L. Puigjaner, *Ind. Eng. Chem. Res.*, **42**, 434 (2003).
6. P. Parthasarathy and S. Narayanan, *Korean J. Chem. Eng.*, **32**, 2236 (2015).
7. T. R. Rao and A. Sharma, *Energy*, **23**, 973 (1998).
8. K. Raveendran, A. Ganesh and K. C. Khilar, *Fuel*, **75**, 987 (1996).
9. H. Yang, R. Yan, H. Chen, D. H. Lee and C. Zheng, *Fuel*, **86**, 1781 (2007).
10. G. Zhu, X. Zhu, Z. Xiao and F. Yi, *J. Anal. Appl. Pyrol.*, **94**, 126 (2012).
11. S. Deguchi, K. Tsujii and K. Horikoshi, *Chem. Commun.*, **31**, 3293 (2006).
12. S. H. Kim, C. M. Lee and K. Kafle, *Korean J. Chem. Eng.*, **30**, 2127 (2013).
13. S. Wang, Y. Du, W. Zhang, X. Cheng and J. Wang, *Korean J. Chem. Eng.*, **31**, 1786 (2014).
14. P. R. Patwardhan, J. A. Satrio, R. C. Brown and B. H. Shanks, *J. Anal. Appl. Pyrol.*, **86**, 323 (2009).
15. M. J. Antal, G. Varhegyi and E. Jakab, *Ind. Eng. Che. Res.*, **37**, 1267, (1998).
16. M. J. Antal and G. Varhegyi, *Ind. Eng. Chem. Res.*, **34**, 703 (1995).
17. G. Varhegyi, E. Jakab and M. J. Antal, *Energy Fuel*, **8**, 1345 (1994).
18. A. G. Bradbury, Y. Sakai and F. Shafizadeh, *J. Anal. Appl. Pyrol.*, **23**, 3271 (1979).
19. R. K. Agrawal, *Can. J. Chem. Eng.*, **66**, 413 (1988).
20. C. Di Blasi, *Prog. Energy Combust.*, **34**, 47 (2008).
21. S. Chayaporn, P. Sungsuk, S. Sunphorka, P. Kuchonthara, P. Piumsomboon and B. Chalermsinsuwan, *Korean J. Chem. Eng.*, **32**, 1081 (2015).
22. S.-S. Kim, J. Kim, Y.-H. Park and Y.-K. Park, *Bioresour. Technol.*, **101**, 9797 (2010).
23. S.-S. Kim and S. H. Kim, *Fuel*, **79**, 1943 (2000).
24. Y.-H. Park, J. Kim, S.-S. Kim and Y.-K. Park, *Bioresour. Technol.*, **100**, 400 (2009).
25. M. R. Othman, Y.-H. Park, T. A. Ngo, S.-S. Kim, J. Kim and K. S. Lee, *Korean J. Chem. Eng.*, **27**(1), 163 (2010).
26. G. H. Choi, S.-S. Kim, J. Kim, D. S. Joo and J. G. Lee, *Appl. Chem. Eng.*, **22**, 508 (2011).
27. S. Ouajai and R. Shanks, *Polym. Degrad. Stabil.*, **89**, 327 (2005).
28. J. Caballero, J. Conesa, R. Font and A. Marcilla, *J. Anal. Appl. Pyrol.*, **42**, 159 (1997).
29. S.-S. Kim and F. A. Agblevor, *Waste Manage.*, **27**, 135 (2007).
30. S. Maiti, S. Purakayastha and B. Ghosh, *Fuel*, **86**, 1513 (2007).
31. R. Soysa, Y. S. Choi, S. K. Choi, S. J. Kim and S. Y. Han, *Korean J. Chem. Eng.*, **33**, 603 (2016).
32. D. Vamvuka, E. Kakaras, E. Kastanaki and P. Grammelis, *Fuel*, **82**, 1949 (2003).
33. G. Wang, W. Li, B. Li and H. Chen, *Fuel*, **87**, 552 (2008).
34. H. J. Park, Y.-K. Park, J.-I. Dong, J.-S. Kim, J.-K. Jeon, S.-S. Kim, J. Kim, B. Song, J. Park and K.-J. Lee, *Fuel Process. Technol.*, **90**, 186 (2009).
35. E. H. Lee, R. Park, H. Kim, S. H. Park, S.-C. Jung, J.-K. Jeon, S. C. Kim and Y.-K. Park, *J. Ind. Eng. Chem.*, In Press (2016).
36. T. A. Le, H. V. Ly, J. Kim, S.-S. Kim, J. H. Choi, H.-C. Woo and M. R. Othman, *Chem. Eng. J.*, **250**, 157 (2014).
37. J. H. Ko, R. S. Park, J. K. Jeon, D. H. Kim, S. C. Jung, S. C. Kim and Y. K. Park, *J. Ind. Eng. Chem.*, **32**, 109 (2015).
38. A. Ross, J. Jones, M. Kubacki and T. Bridgeman, *Bioresour. Technol.*, **99**, 6494 (2008).